Supplementary Information

The lipid kinase PI4KIIIβ preserves lysosomal identity

Sunandini Sridhar, Bindi Patel, David Aphkhazava, Fernando Macian, Laura Santambrogio, Dennis Shields[†] and Ana Maria Cuervo

---

Supplementary information

- **Supplemental Figure Legends**
- **Supplemental Figures**
- **Supplemental Movie Legends**
- **Supplemental Materials and Methods**
- **Supplemental References**

Supplemental Figure Legends

Figure S1. LAMP1 dynamics are altered in PI4KIIIβ-deficient cells. (**A**) Secretion of ^{35}S-labeled proteins in mouse fibroblasts control (Ctr) or stably knocked down for PI4KIIIβ (PI4KIIIβ(-)). Values are expressed in counts in the media normalized to 10 μg protein and are mean±s.e.m. (n=3). (**B-D**) Live cell microscopy in the same cells upon transfection with yellow fluorescence protein (YFP) tagged LAMP1. (**B**) Representative still images. Arrows: LAMP1 tubules. Brackets: tubule size (μm). (**C**) Higher magnification example of tubular structures. (**D**) Sequential frames at 9s intervals (inverted grayscale). (**E-G**) LAMP1 dynamics in a second knock-down for PI4KIIIβ of lower efficiency. (**E**) Immunoblot for the indicated proteins of mouse fibroblasts control or subjected to knock-downs for PI4KIIIβ of different efficiency (sh(1) 48% efficiency and sh(2) 72% efficiency). (**F**) Live cell microscopy upon transfection of control and sh(1) cells with yellow fluorescence protein (YFP) tagged LAMP1. Brackets: tubules. (Similar analysis for sh(2) is shown in panel B). (**G**) Immunofluorescence for LAMP1 (red) in control and sh(1) cells. Arrows: LAMP1 clusters. (Similar analysis for sh(2) is shown in Fig. 2A).

Figure S2. Depletion of PI4KIIIβ alters the morphology and cellular distribution of LAMP1 positive compartments. (**A**) Electron microscopy in mouse fibroblasts control (ctr) or stably knocked down for PI4KIIIβ (PI4KIIIβ(-)). Bottom: higher magnification images. Arrows: interconnected vesicular compartments. (**B**) Immunogold for LAMP1 in PI4KIIIβ(-) cells. Orange arrow indicates gold outside lysosomal or tubules. Blue arrow indicates tubule labeling. Bottom: quantification of the distribution of gold particles in tubules, cluster compartments and lysosome unrelated regions (other). Values are expressed as percentage and are mean+s.e.m. (n=8). (***P=0.00032 (tubules) and 0.00065 (clusters), t test). (**C,D**) Immunofluorescence for HA (green) and LAMP1 (red) in control cells transiently transfected with wild-type (WT) or kinase dead PI4KIIIβ. (KiD). Arrows: LAMP1 clusters. Representative single channel and merged images (**C**) and average

number and size of LAMP1-positive puncta (**D**). Values are mean±SE of >25 cells (n=3) (****P*=0.00012 (number) and 0.0032 (size), *t* test).

Figure S3. LAMP1 dynamics relative to Golgi and endosomal markers in PI4KIIIβ-deficient cells. (**A**) Live cell microscopy upon transient transfection of control cells with red fluorescence tagged LAMP1 and the indicated green fluorescence tagged Golgi-markers. Individual and merged channels are shown. (**B**) Live cell microscopy upon transient transfection of control cells and cells stably knocked down for PI4KIIIβ with red fluorescence tagged LAMP1 and the indicated fluorescent endosomal markers. Individual and merged channels are shown. Arrows: LAMP1 tubules (white) and Golgi markers (pink). (**C**) Immunofluorescence for LAMP1 (red) and the indicated endosomal markers (green) in control and PI4KIIIβ(-) cells. Insets: high magnification images. (**D**). Average percent colocalization between LAMP1 and the indicated endosomal markers. Values are mean±s.e.m. of n>25 cells (n=3). (**E**) Immunoblot for the indicated proteins in homogenate (Hom), early endosome (EE) and late endosome (LE) fractions isolated from rat liver.

Figure S4. The lysosome is the origin of the LAMP1 tubular structures observed in PI4KIIIβ-deficient cells. (**A**) Live cell microscopy upon transient transfection of PI4KIIIβ(-) cells with red fluorescence tagged LAMP1 and the indicated lysosomal dyes (green). (**B**) Live cell imaging of control cells expressing LAMP1-RFP and stained with the indicated dyes or expressing mCherry-GFP tagged LC3. Merged channels are shown. (**C**) Average percent colocalization between LAMP1 and different lysosomal markers. Values are mean±s.em.of n>25 cells (n=3) (****P*=0.00021 (dextran), 0.000026 (LysoTracker), 0.000042 (Pepstatin A) and 0.000028 (Cath D), *t* test). (**D**) Live cell imaging of LAMP1-RFP and the autophagosome-marker GFP-LC3 in cells control or stably knocked down for PI4KIIIβ (PI4KIIIβ(-)). Arrows: LAMP1 tubulation (white) and LC3-positive compartments (pink).

Figure S5. Changes in Golgi exit and in the lysosomal compartment in PI4KIIIβ-deficient cells. (**A**) Kinetics of LAMP1 Golgi exit in mouse fibroblasts control (Ctr) or stably knockdown for

PI4KIIIβ (PI4KIIIβ(-). *Top:* immunoblot for LAMP1 in lysosome enriched fractions isolated after a TGN (20°C, 4h) block (blk) or a 2h release (rls) at 37°C. *Bottom:* Average changes in the lysosomal levels of LAMP1 in treated relative to untreated conditions. Values are mean+s.e.m. (n= 3) (**B**) Kinetics of VSVG Golgi exit in mouse fibroblasts control (Ctr) or stably knockdown for PI4KIIIβ (PI4KIIIβ(-) transiently expressing ts045VSVG-GFP after treatment with a TGN block (20°C, 4h) and release (32°C, 45 min). *Top:* representative images; *Bottom:* Quantification of >25 cells. Values are mean+s.e.m. (n=3) (**C**) Distribution of lysosomal proteins upon subjecting lysates of control and PI4KIIIβ(-) cells to continuous sucrose density gradients. Top: representative immunoblots. Bottom: percentage of total protein recovered in each fraction. Arrows: intermediate (int) and mature (m) forms of CathD (black); shifted fractions in PI4KIIIβ(-) cells (red). (**D**) Immunofluorescence for LAMP1 (red) and PI4KIIIβ (green) in lysosomes isolated from rat liver. Individual and merged channels and percentage of colocalization are shown. Arrows: colocalization. (**E**) Electron microscopy and immunogold for PI4KIIIβ in the same lysosomes. Bottom: individual lysosomes at higher magnification.

Figure S6. Characteristics of the lysosome-associated PI4KIIIβ. (**A**) Immunoblot for the indicated proteins in homogenate (Hom) and lysosomes (Lys) isolated from mouse fibroblasts (3 different preparations are shown). (**B**) Immunoblot for the indicated proteins in homogenate (Hom) and lysosome-enriched fractions (Lys-enr) isolated from mouse fibroblasts untreated or treated with leupeptin (Leup.) to block lysosomal degradation. (**C,D**) Immunoblot for the indicated proteins of rat liver lysosomes incubated with (**C**) increasing concentrations of trypsin. *Right*: Percentage of protein degraded relative to untreated samples. Values are mean±s.e.m. (n=3) or (**D**) the indicated buffers of increasing stringency followed by centrifugation to recover the protein still associated to the lysosomal membrane. *Bottom*: Percentage of protein remaining after the washes relative to that in untreated (MOPS buffer:control) samples. Values are mean±s.e.m. (n=3). (**E**) Immunoblot for the indicated proteins in the fractions obtained upon detergent extraction of rat liver lysosomes and

floatation in discontinuous sucrose gradients. DR: detergent-resistant; INT: intermediate region; SOL: detergent-soluble. *Bottom*: Quantification of the percentage of lysosome-associated protein detected in the detergent-resistant region. Values are average of two samples. (**F**) Immunoblot for GFP of lysosomes incubated alone (lane 2) or with cytosol from mouse fibroblasts expressing FAPP-PH-GFP (+). Inp: input. Lanes 3-5 show lysosomes isolated from three different animals.

Figure S7. PI4KIIIβ associates with vesicular compartments and trafficking determinants. (**A**) Electron microscopy and immunogold for PI4KIIIβ of cytosolic vesicles isolated by sequential centrifugation in the 500,000g pellet (500K). Insets show individual vesicles. (**B**) Proteomics of the PI4KIIIβ-enriched cytosolic vesicles purified from the 500K fraction. Left: immunoblot for PI4KIIIβ and silver staining of the input and immunopurified (IP) vesicular fraction. Right: proteins identified in this fraction by the proteomic analysis grouped in families.

Figure S8. Function of lysosomal PI4K and PIP5Ks in the control of lysosomal efflux. (**A**) RT-PCR for PIP5K1A, PIP5K1B and PI4KIIIβ mRNA in single and double knock-downs cells (values are expressed relative to control cells and are average of 2 samples); percentage of knockdown is indicated. (**B**) Live cell microscopy in fibroblast PI4KIIIβ (-) and PIP5K1B(-) transiently transfected with red fluorescence tagged LAMP1 and pepstatin A when serum was added for 1h after deprivation for 12h (Serum-/Refeeding). Merged (left) and individual channels (right) are shown. This cell is representative of a more pronounced phenotype to the one shown in main Fig. 8B observed in about 20% of the cells. (**C**) Live cell microscopy in fibroblast control or knockdown for PIP5K1B or PIP5K1A alone or in combination with PI4KIIIβ knockdown transiently transfected with red fluorescence tagged LAMP1 and maintained in the presence of serum. Reversed black and white images correspond to the boxed areas at higher magnification.

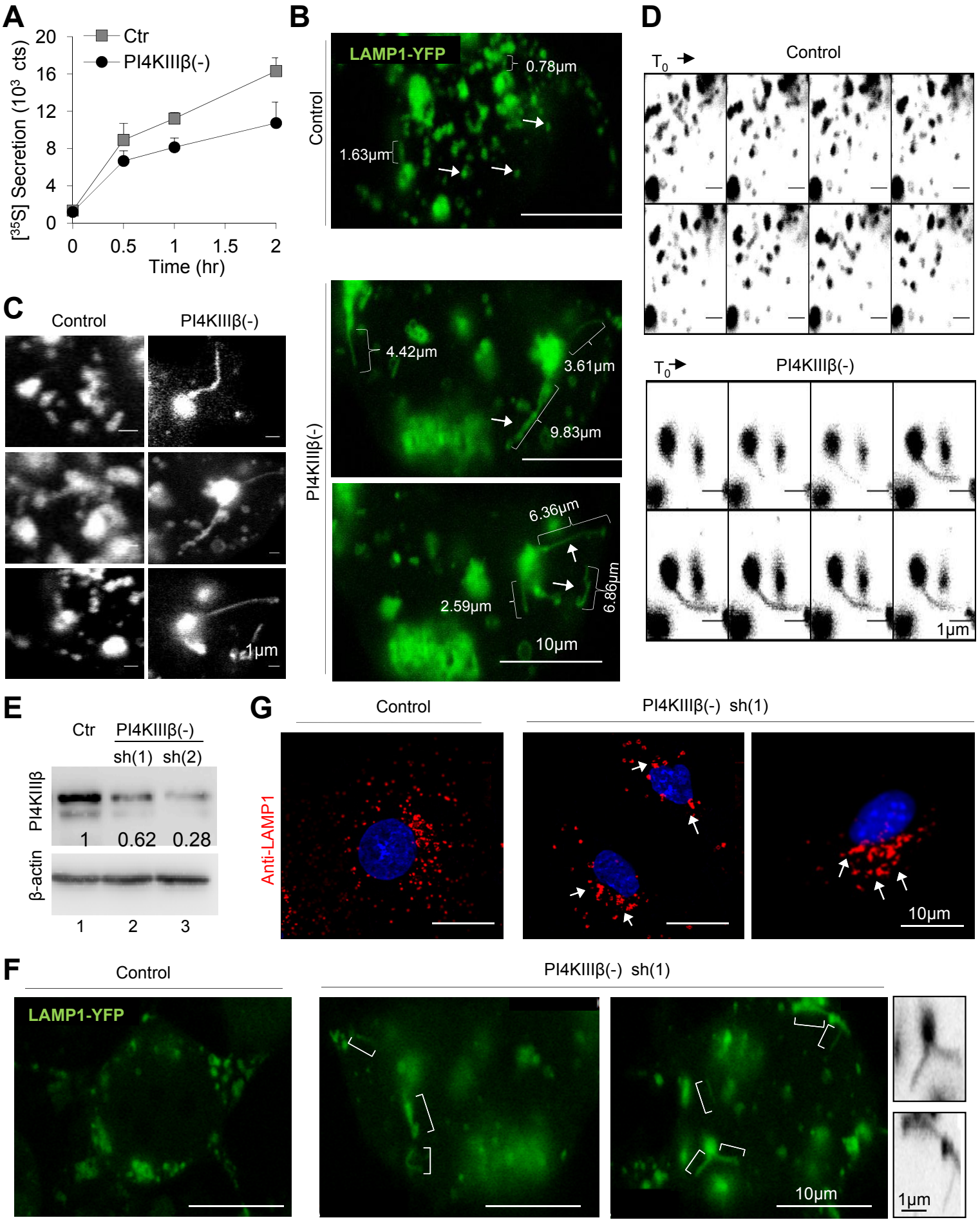
A
Ctr
PI4KIIIβ(-)
[35S] Secretion (10³ cts)
Time (hr)
B
LAMP1-YFP
Control
PI4KIIIβ(-)
0.78μm
1.63μm
4.42μm
3.61μm
9.83μm
6.36μm
6.86μm
2.59μm
10μm
C
Control
PI4KIIIβ(-)
1μm
D
Control
PI4KIIIβ(-)
1μm
E
Ctr
PI4KIIIβ(-)
sh(1)
sh(2)
PI4KIIIβ
β-actin
1
0.62
0.28
1
2
3
G
Control
PI4KIIIβ(-) sh(1)
Anti-LAMP1
10μm
F
Control
PI4KIIIβ(-) sh(1)
LAMP1-YFP
10μm
1μm

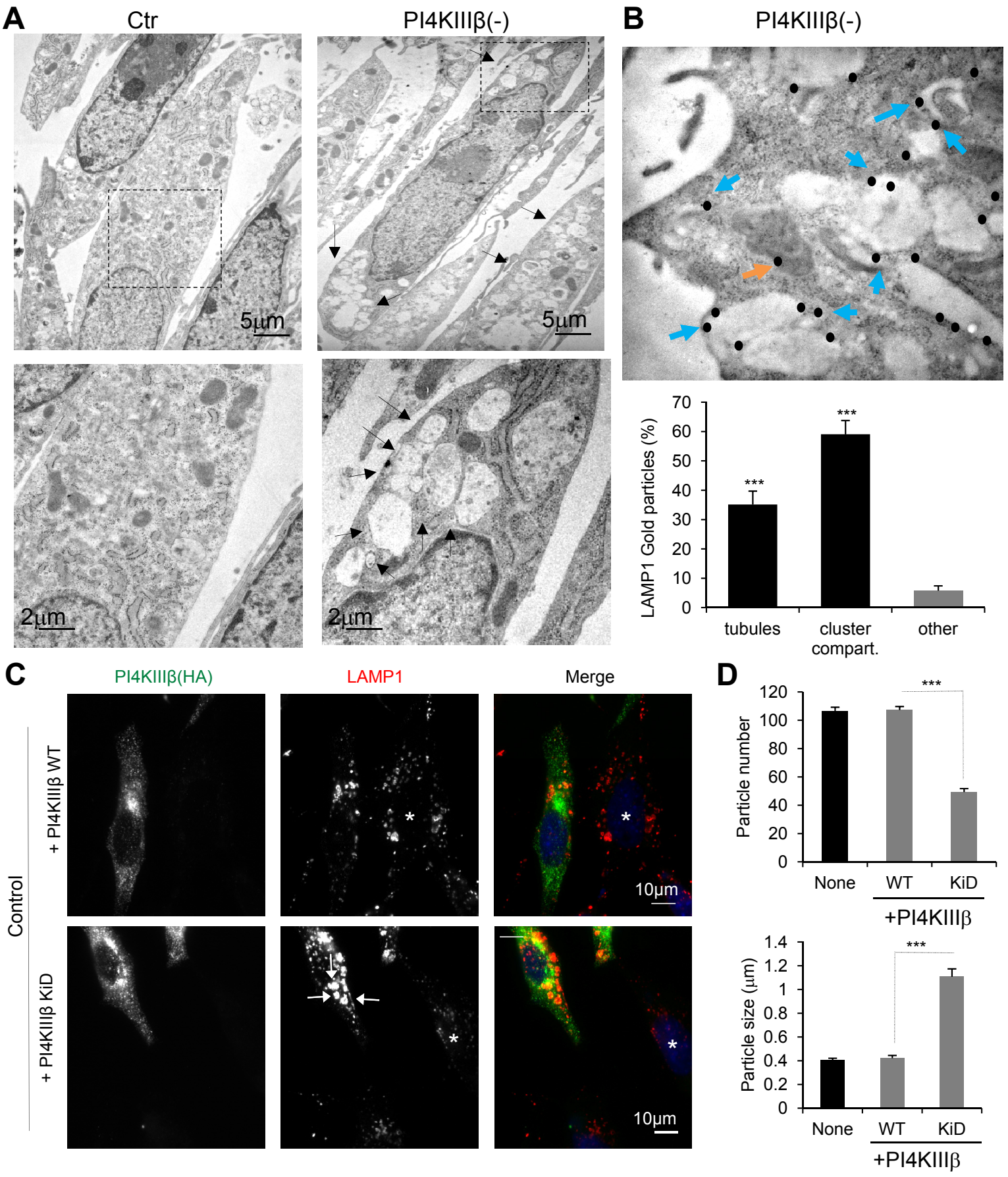
A
Ctr
PI4KIIIβ(-)
5μm
5μm
2μm
2μm
B
PI4KIIIβ(-)
LAMP1 Gold particles (%)
70
60
50
40
30
20
10
0
***
***
tubules
cluster compart.
other
C
PI4KIIIβ(HA)
LAMP1
Merge
Control
+ PI4KIIIβ WT
+ PI4KIIIβ KiD
10μm
10μm
D
Particle number
120
100
80
60
40
20
0
***
None
WT
KiD
+PI4KIIIβ
Particle size (μm)
1.4
1.2
1
0.8
0.6
0.4
0.2
0
***
None
WT
KiD
+PI4KIIIβ

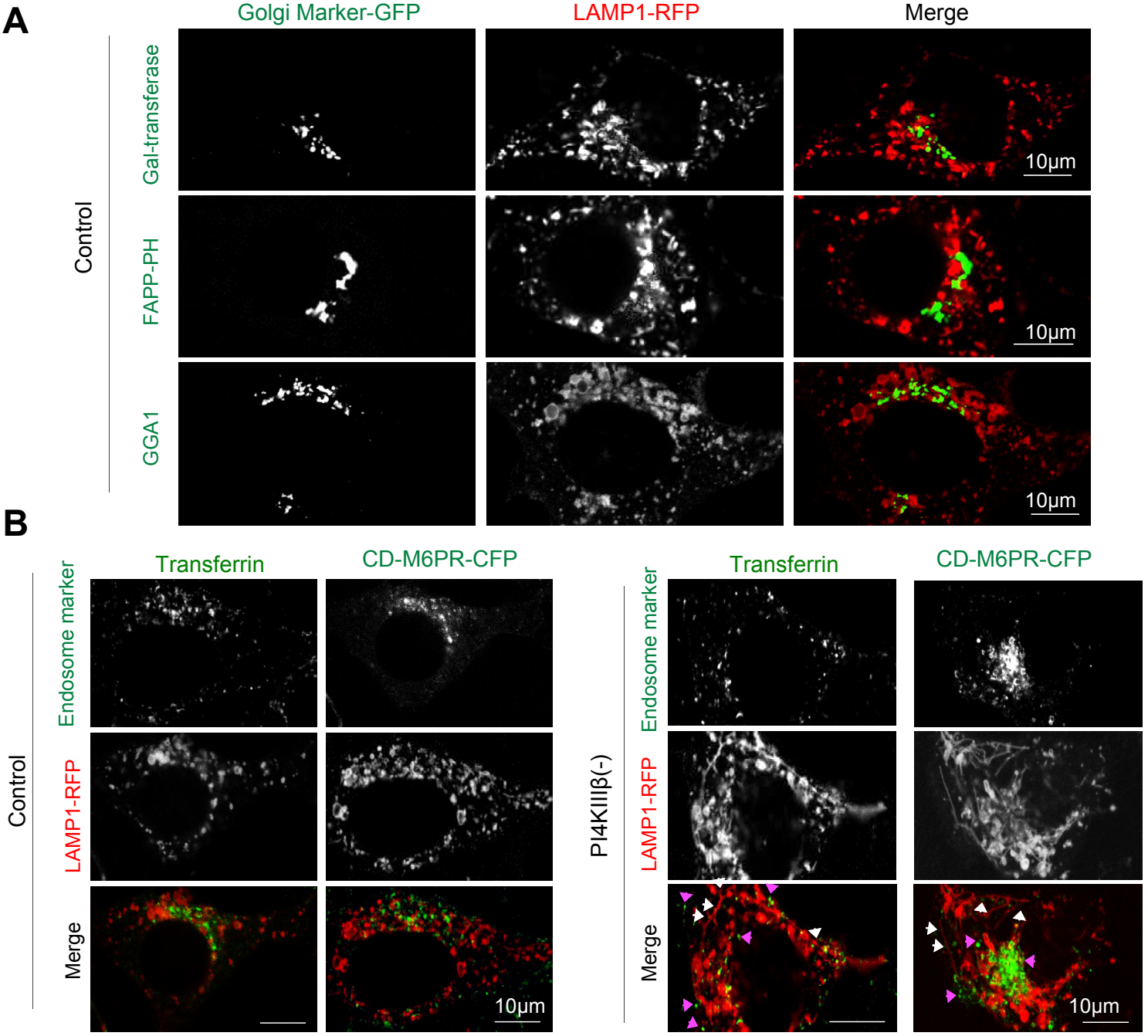
A
Golgi Marker-GFP
LAMP1-RFP
Merge
Control
Gal-transferase
FAPP-PH
GGA1
10μm
B
Transferrin
CD-M6PR-CFP
Endosome marker
LAMP1-RFP
Merge
Control
PI4KIIIβ(-)
10μm
C
Rab5-LAMP1
Rab7-LAMP1
Control
PI4KIIIβ(-)
10μm
D
Control
PI4KIIIβ(-)
Percent colocalization
0
5
10
15
20
25
30
35
40
Transferrin
Rab5
Rab7
CD-M6PR

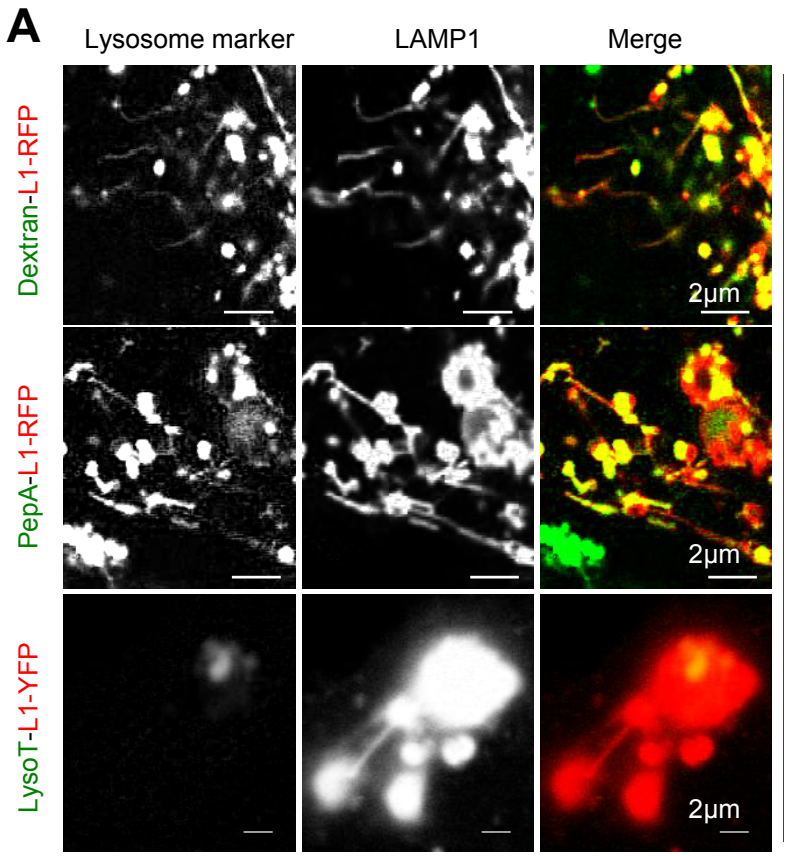
A
Lysosome marker
LAMP1
Merge
Dextran-L1-RFP
PepA-L1-RFP
LysoT-L1-YFP
2μm
2μm
2μm
PI4KIIIβ(-)

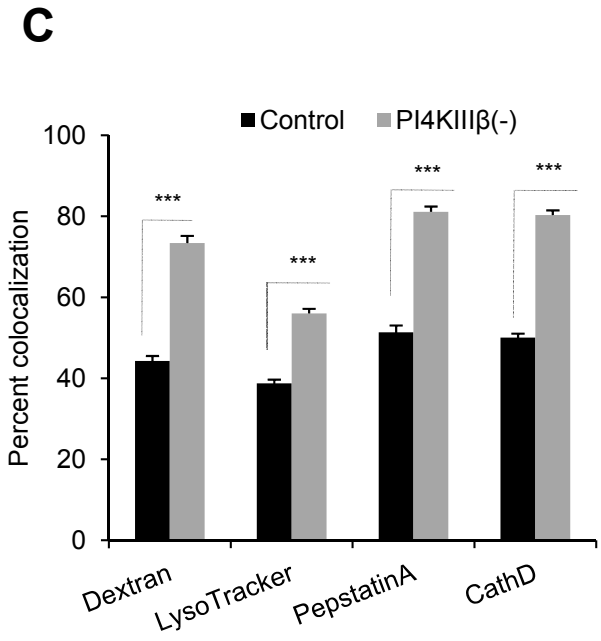
C
Control
PI4KIIIβ(-)
Percent colocalization
100
80
60
40
20
0
***
***
***
***
Dextran
LysoTracker
PepstatinA
CathD

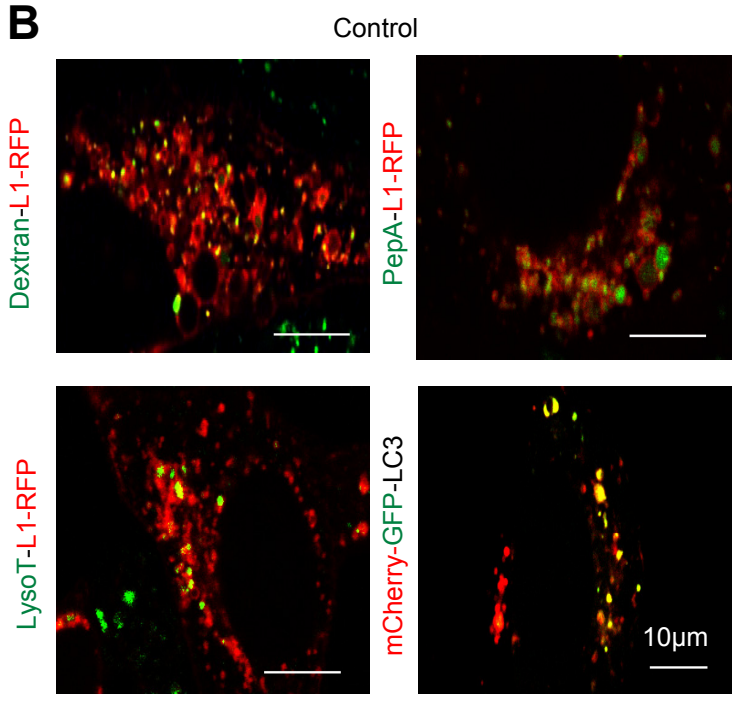
B
Control
Dextran-L1-RFP
PepA-L1-RFP
LysoT-L1-RFP
mCherry-GFP-LC3
10μm

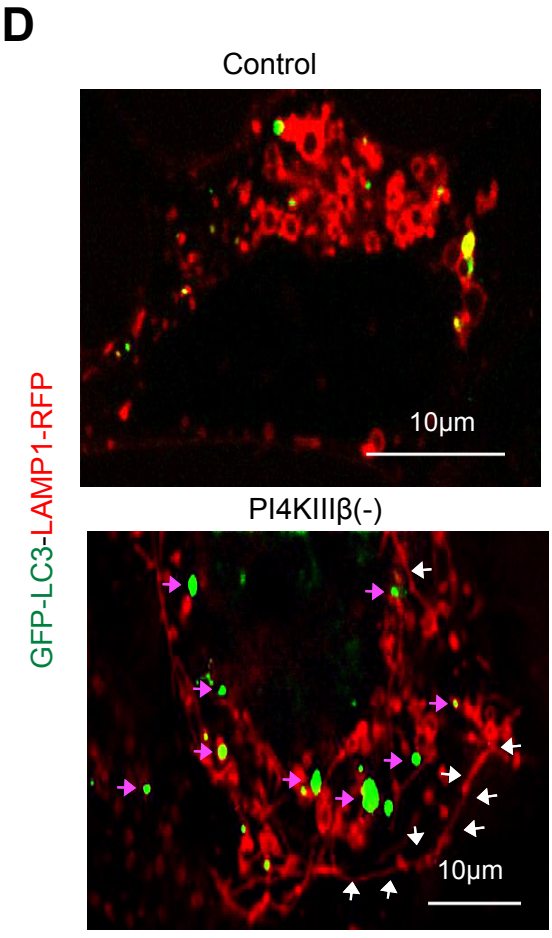
D
Control
PI4KIIIβ(-)
GFP-LC3-LAMP1-RFP
10μm
10μm

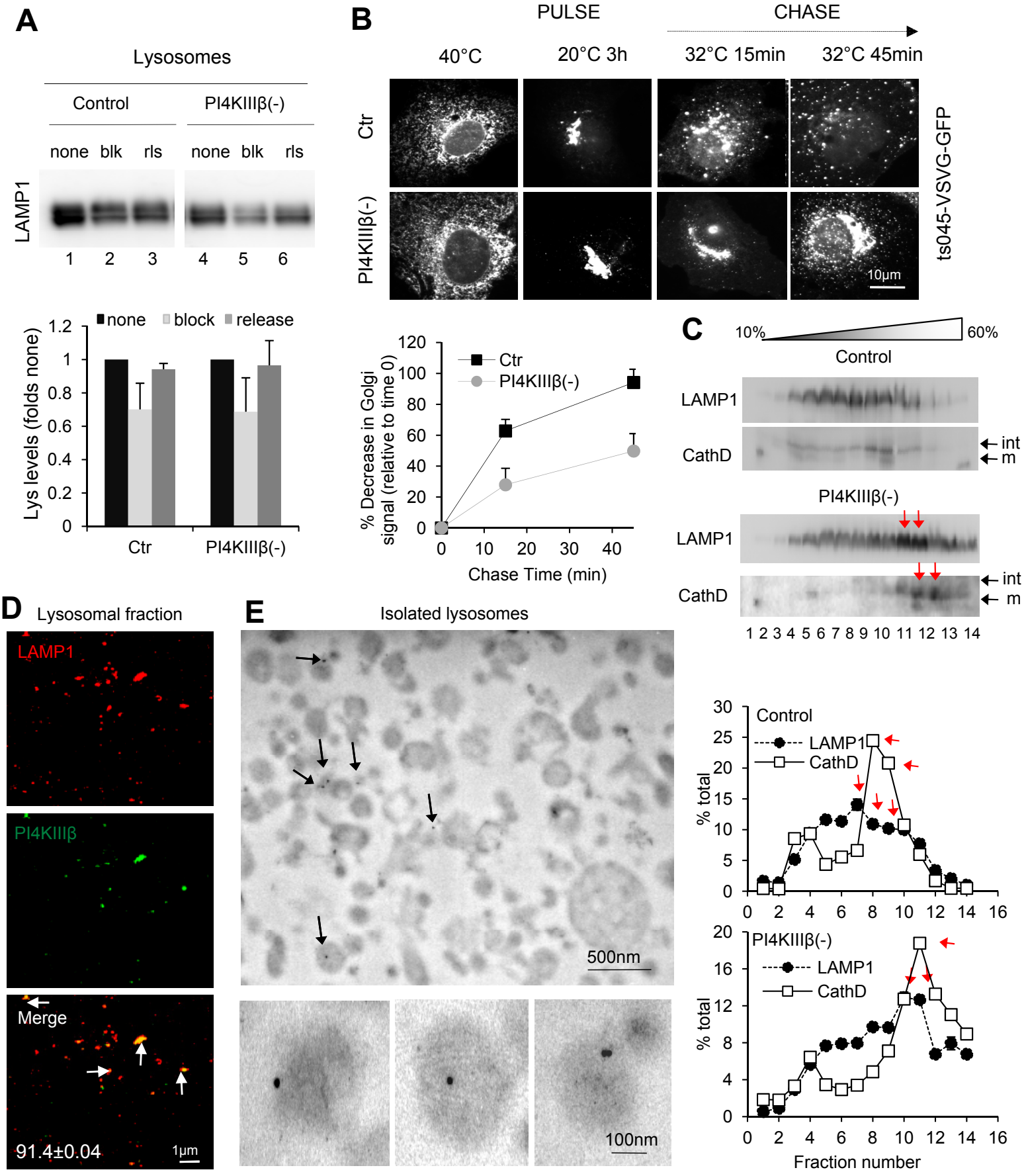
A
Lysosomes
Control
PI4KIIIβ(-)
none blk rls none blk rls
LAMP1
1 2 3 4 5 6
none block release
Lys levels (folds none)
Ctr
PI4KIIIβ(-)
B
PULSE
CHASE
40°C
20°C 3h
32°C 15min
32°C 45min
Ctr
PI4KIIIβ(-)
ts045-VSVG-GFP
10μm
% Decrease in Golgi signal (relative to time 0)
Ctr
PI4KIIIβ(-)
Chase Time (min)
C
10%
60%
Control
LAMP1
CathD
int
m
PI4KIIIβ(-)
LAMP1
CathD
int
m
1 2 3 4 5 6 7 8 9 10 11 12 13 14
D
Lysosomal fraction
LAMP1
PI4KIIIβ
Merge
91.4±0.04
1μm
E
Isolated lysosomes
500nm
100nm
Control
LAMP1
CathD
% total
PI4KIIIβ(-)
LAMP1
CathD
% total
Fraction number

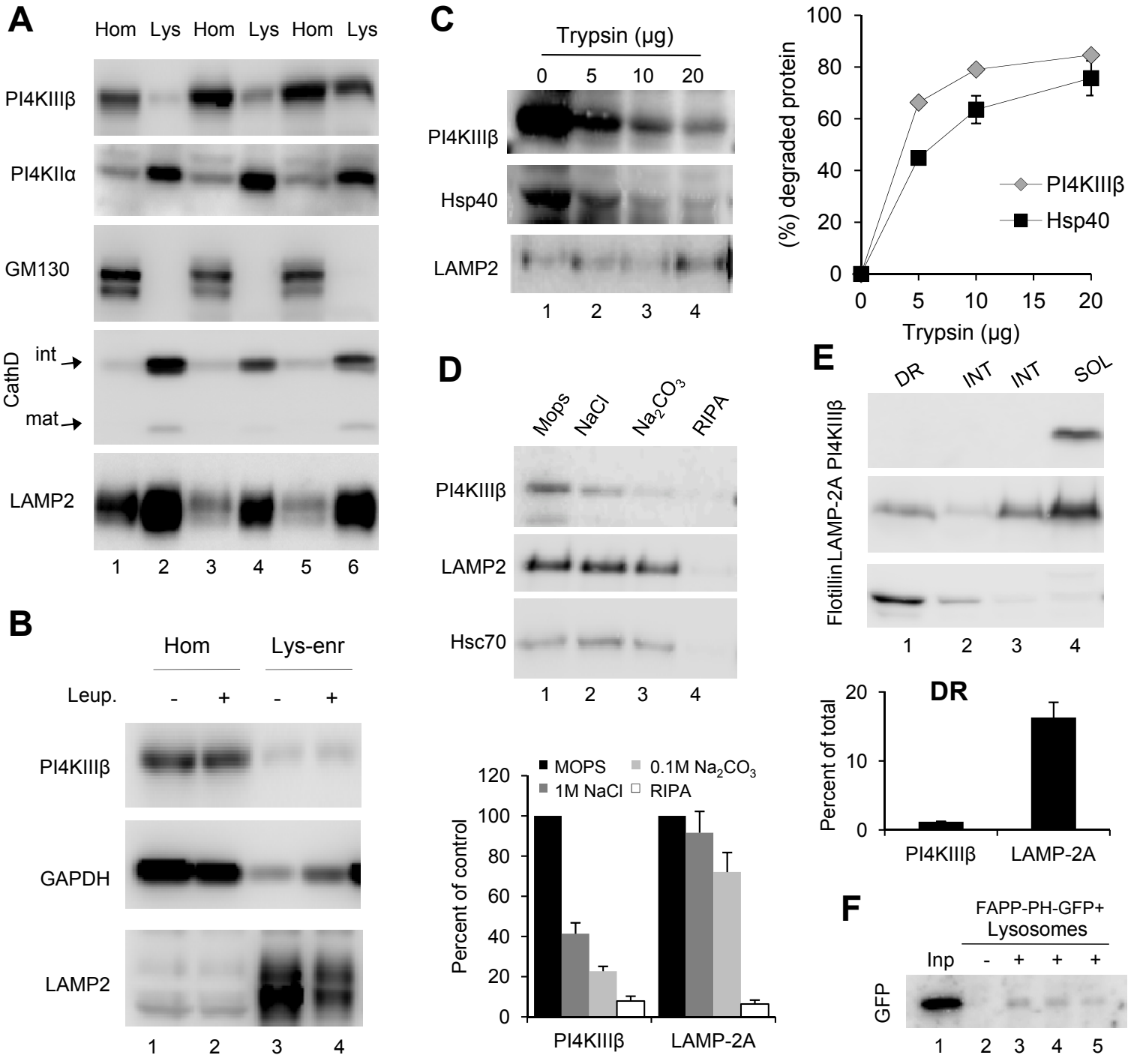
A
Hom Lys Hom Lys Hom Lys
PI4KIIIβ
PI4KIIα
GM130
CathD
int
mat
LAMP2
1 2 3 4 5 6
B
Hom
Lys-enr
Leup. - + - +
PI4KIIIβ
GAPDH
LAMP2
1 2 3 4
C
Trypsin (μg)
0 5 10 20
PI4KIIIβ
Hsp40
LAMP2
1 2 3 4
(%) degraded protein
Trypsin (μg)
PI4KIIIβ
Hsp40
D
Mops
NaCl
Na_2CO_3
RIPA
PI4KIIIβ
LAMP2
Hsc70
1 2 3 4
MOPS
0.1M Na_2CO_3
1M NaCl
RIPA
Percent of control
PI4KIIIβ
LAMP-2A
E
DR
INT
INT
SOL
Flotillin
LAMP-2A
PI4KIIIβ
1 2 3 4
DR
Percent of total
PI4KIIIβ
LAMP-2A
F
FAPP-PH-GFP+ Lysosomes
Inp - + + +
GFP
1 2 3 4 5

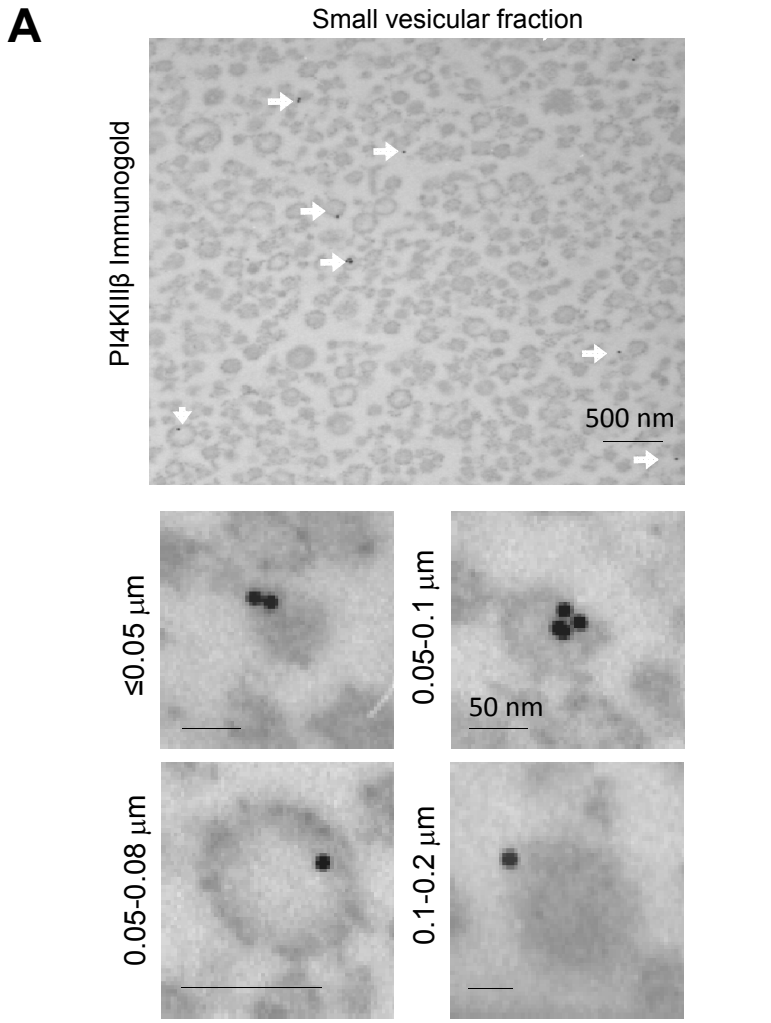

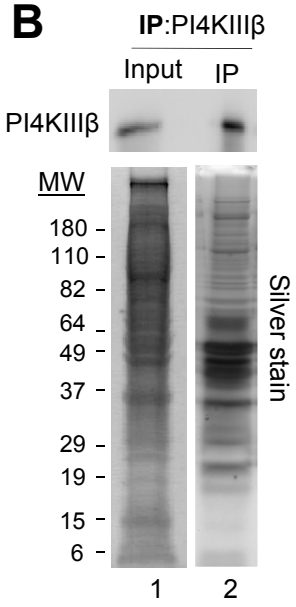

PROTEIN FAMILY	PI4KIIIβ-ENRICHED VESICLES	
Adaptors Clathrin transport	AP3B1	AP3S1
	AP3D1	AP3S2
	AP3M1	CLTC
Vesicle fission/ fusion	RAB5C	RAB11B
	RAB7A	NSF
	RAB9A	
Motor proteins	KIF13B	DCTN1
	KIF21A	DCTN2
	KIF5B	DCTN3
	NM1L	DCTN5
	DYNC1H1	
Lysosomal proteins	CathA	Cath L
	Cath B	ATP6V1

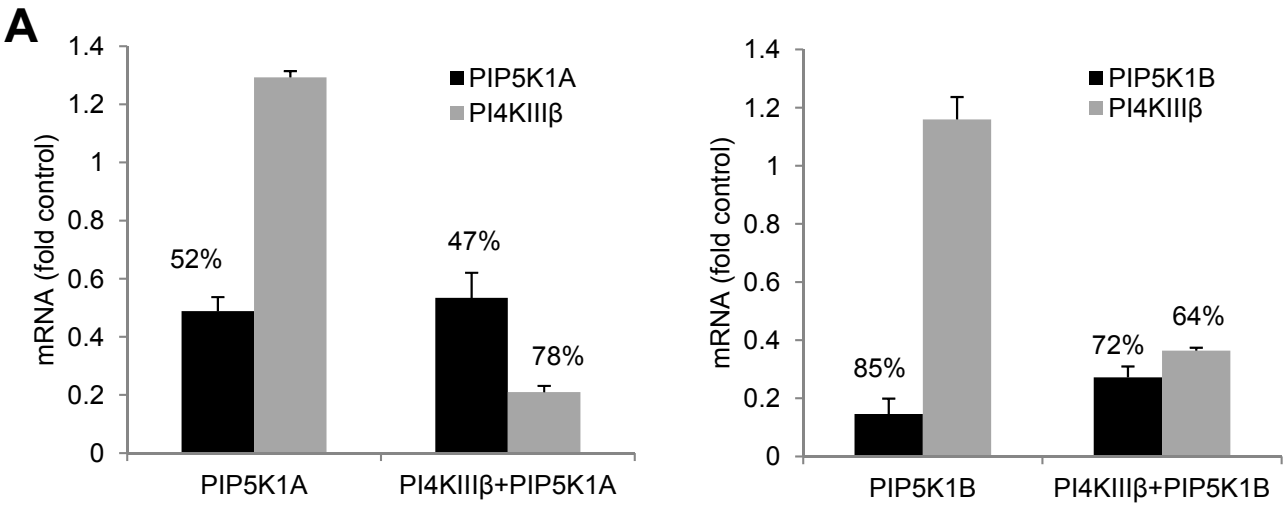
A
mRNA (fold control)
1.4
1.2
1
0.8
0.6
0.4
0.2
0
PIP5K1A
PI4KIIIβ
52%
47%
78%
PIP5K1A
PI4KIIIβ+PIP5K1A
PIP5K1B
PI4KIIIβ
85%
72%
64%
PIP5K1B
PI4KIIIβ+PIP5K1B

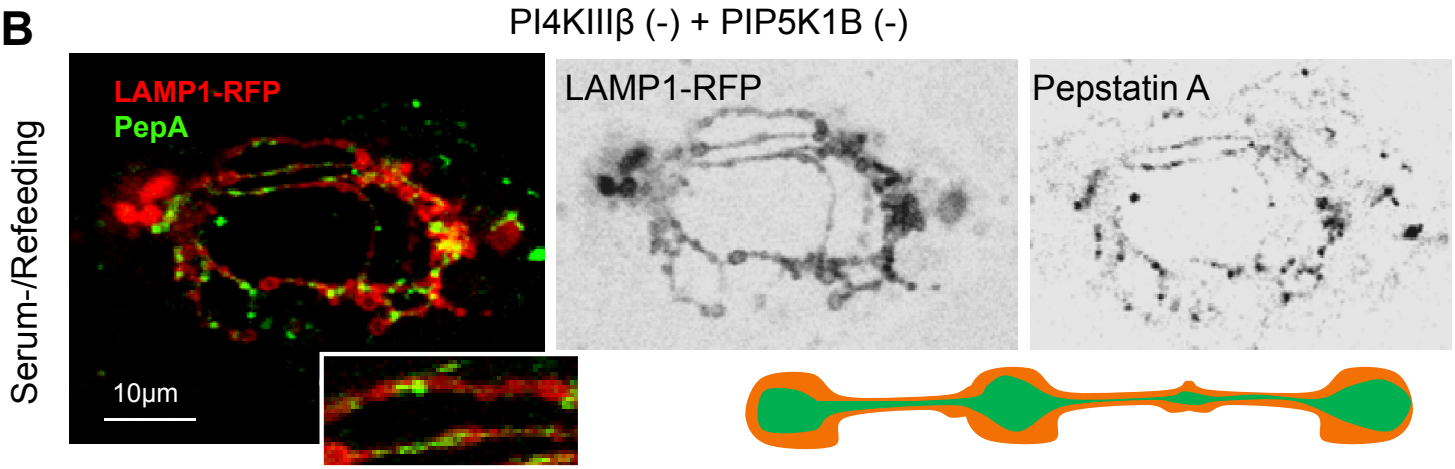
B
PI4KIIIβ (-) + PIP5K1B (-)
Serum-/Refeeding
LAMP1-RFP
PepA
10μm
LAMP1-RFP
Pepstatin A

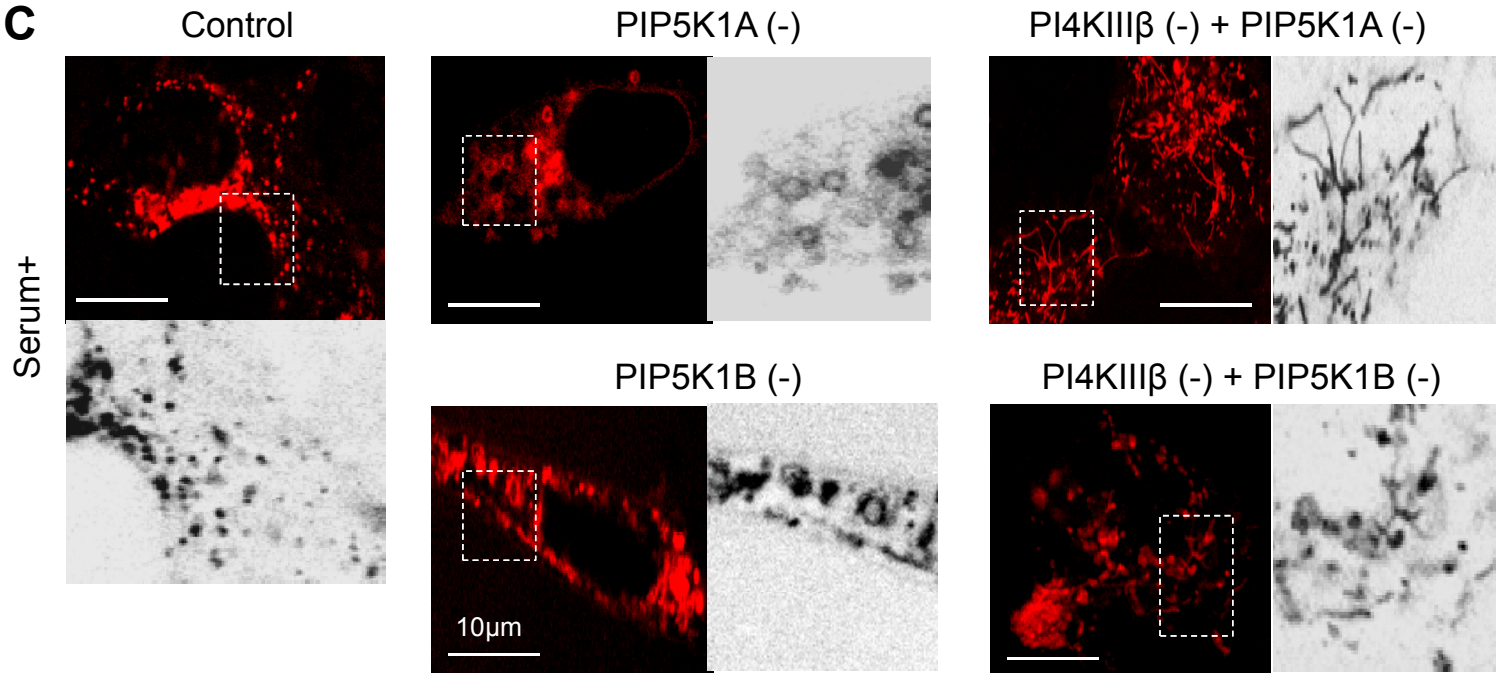
C
Control
PIP5K1A (-)
PI4KIIIβ (-) + PIP5K1A (-)
Serum+
PIP5K1B (-)
PI4KIIIβ (-) + PIP5K1B (-)
10μm

Supplemental Movie Legends

Movie S1. LAMP1 dynamics in control and PI4KIIIβ-defective cells and effect of nocodazole. Scale bar: 10μm. Please press CTR+L for continuous looping.

Movie S2. Effect of expression of human wild-type and kinase-dead PI4KIIIβ on LAMP1 dynamics in control and PI4KIIIβ-defective cells. Scale bar: 10μm. Please press CTR+L for continuous looping.

Movie S3. LAMP1 dynamics relative to Golgi markers in PI4KIIIβ-defective cells and effect of brefeldin A. Scale bar: 10μm. Please press CTR+L for continuous looping.

Movie S4. LAMP1 dynamics relative to endosomal markers in PI4KIIIβ-defective cells. Scale bar: 10μm. Please press CTR+L for continuous looping.

Movie S5. LAMP1 dynamics relative to lysosomal markers in PI4KIIIβ-defective cells. Scale bar: 10μm. Please press CTR+L for continuous looping.

Movie S6. LAMP1, clathrin and Rab9 dynamics in PI4KIIIβ-defective cells. Scale bar: 10μm. Please press CTR+L for continuous looping.

Movie S7. LAMP1 dynamics relative to pepstatin A in control cells and PI4KIIIβ-defective cells in basal and starvation/refeeding conditions. Scale bar: 10μm. Insets scale bars: 2μm. Please press CTR+L for continuous looping.

Movie S8. LAMP1 dynamics relative to pepstatin A in cells knocked-down for PIP5K1A or PIP5K1B alone or in combination with PI4KIIIβ knockdown in starvation/refeeding conditions. Scale bar: 10μm. Insets scale bars: 2μm. Please press CTR+L for continuous looping.

Supplemental Materials and Methods

Animals, Cell culture and treatments. Adult male Wistar rats (200–250 g) and C57BL/6 male mice were used. NIH3T3, COS7 and HEK293T cell lines were purchased from American Type Culture Collection (Manassas, VA). Except where indicated, all cells were cultured in a 37^0C incubator with 5% CO_2 in complete DMEM medium (GIBCO) supplemented with 10% heat-inactivated newborn calf serum (NCS) and penicillin/streptomycin/Fungizone®. Where mentioned, cells were treated with 33μM nocodazole (Calbiochem, San Diego, CA), 5μg/ml BFA (Calbiochem), 20mM ammonium chloride plus 100μM leupeptin (Fisher) for the indicated times. Where mentioned, lysosomal fractions were treated with lambda protein phosphatase (NEB) according to manufacturer's instructions. All studies were approved by the Animal Care and Use Committee of the Albert Einstein College of Medicine and followed the National Institutes of Health guidelines for animal care.

Antibodies, cDNA constructs and transfection. The following antibodies were used in this study: mouse PI4KIIIβ (BD biosciences), rabbit PI4KIIIβ (Millipore), rabbit PI4KIIIα, rabbit PI4KIIβ and rabbit PI4KIIα antibodies were obtained from the laboratory of the latest D. Shields, Albert Einstein College of Medicine. Rabbit antibodies against the cytosolic tail of LAMP-2A and LAMP-2B were developed in our laboratory (Cuervo & Dice, 1996; Zhang & Cuervo, 2008). Rat LAMP1 (1D4B, Developmental Studies Hybridoma Bank), rat LAMP2 (ABL93, Developmental Studies Hybridoma Bank), rabbit V-ATPase (H-180, Santa Cruz), goat CathepsinB (S-12, Santa Cruz), goat CathepsinD (C-20, Santa Cruz), goat CathepsinL (C-18, Santa Cruz), rabbit p62 (Enzo life sciences), mouse E-Cadherin (BD bioscences), mouse NADH:ubiquinone oxidoreductase (generous gift from R.Stanley, Albert Einstein College of Medicine, rat HA (3F10, Roche applied science), mouse GM130 (BD biosceinces), rabbit Rab5 (C8B1, Cell Signalling), rabbit Rab7 (H-50, Santa Cruz) , rabbit Rab9 (FL-201, Santa Cruz), rabbit Rab11

(Invitrogen), mouse GAPDH (Abcam), mouse β-Actin (Abcam), mouse Hsc70 (IgM ,13D3, Novus biologicals), rabbit Hsp40 (Enzo life sciences), mouse Flotillin (BD biosciences), mouse ClathrinHC (BD biosciences), mouse AP-1 (γ-adaptin, BD), mouse AP-2 (α-adaptin, BD biosciences), mouse AP-3 (δSA4, Developmental Studies Hybridoma Bank), rabbit Kif13b (Aviva Systems Biology), mouse Vti1b (BD biosciences). The following plasmids were used in this study: rat LAMP1-RFP (plasmid 1817) (Sherer et al, 2003), rat LAMP1-YFP (plasmid 1816) (Sherer et al, 2003), and human GFP-LC3 (plasmid 24920) (Lee et al, 2008) constructs were purchased from Addgene plasmid sharing database. The fluorescence proteins used in the tagging correspond to the modified variants of RFP and YFP (mRFP1 and EYFP) that remain as monomeric proteins upon expression. Human Clathrin (light chain)-GFP, human CD-M6PR-CFP, human GGA1-GFP (Puertollano et al, 2003) were provided by J. Bonifacino, NICHD, NIH. A. Muesch, Albert Einstein College of Medicine, provided galactosyltransferase-GFP and Sialyltransferase-RFP constructs. human FAPP-PH-GFP, HA- human PI4KIIIβWT, human HA-PI4KIIIβ(D656A)KD and human GFP-PI4KIIIβWT constructs were from the late D.Shields, Albert Einstein College of Medicine. mcherry-GFP-LC3 tandem tagged construct was obtained from Addgene (plasmid 22418 deposited by Dr. J. Debnath). Cells were transfected with cDNA constructs using Lipofectamine™ 2000 reagent (Invitrogen) according to manufacturer's instructions.

Real-time PCR. Quantitative real time PCR was used to determine changes in mRNA levels using the TaqMan One-Step RT-PCR Master Mix reagent (Applied Biosystem). Relative transcript levels were analyzed by real-time PCR in 20µl reaction volume on 96-well plates, using StepOne Plus Real-Time PCR Cycler (Applied Biosystems). The expression levels of LAMP1, LAMP-2A, CathepsinB, CathepsinD and PI4KIIIβ in different samples were normalized to those of β-Actin in the same samples. The following primer pairs were used for RT-PCR analysis: mouse LAMP1 Fwd:5'- TAGTGCCCACATTCAGCATCTCCA-3' Rvs: 5'-TTCC

ACAGACCCAAACCTGTCACT-3'; mouse LAMP-2A fwd: 5'-AGGTGCTTTCTGTGTCTAGAG CGT-3' Rvs: 5'-AGAATAAGTACTCCTCCCAGAGCTGC ; mouse CathepsinB fwd: 5'-TCTG AAGAAGCTGTGTGGCACTGT-3' Rvs: 5'-TAATCTGTCCAATGGTCGGGCAGT-3'; mouse Cathepsin D fwd: 5'-CCAAGTTTGATGGCATCTTGGGCA-3" Rvs: 5'-TGGAGTCAGTGCCACCAAGCATTA-3'; mouse PI4KIIIβ fwd: 5'-TTGCAAGTCAAGGACAGGCACAAC-3' Rvs: 5'-TAAAGGCTGATGTCTCGAAGCCCA-3'; mouse PIP5K1A fwd: 5'-GGAGAAAGGCTCCTGCTTTAT-3' Rvs: 5'- GACCAGTGCTTTCCAAGAGT ; mouse PIP5K1B fwd: 5'- CCTGAAAGGCTCCACATACAA-3' Rvs: 5'-CAGGAAGTCCAGGTCCTTAAAC-3'.

Live cell microscopy and image analysis. Live cell imaging was performed 24h post-transfection using a microscope (TCS SP5) equipped with a motorized x-y stage for multiple position finding (Leica) and with an 8,000-Hz resonant scanner (lenses: HCX Plan Apo CS 63.0× NA 1.40 oil). Treated/pre-loaded (where mentioned) or untreated cells were imaged on poly-L-lysine–coated MaTek chambers at 37°C in a CO_2-enriched atmosphere in recording medium (DMEM without Phenol red (GIBCO), 10% NCS, 3.7mg/ml $NaHCO_3$, and 25mM HEPES, pH 7.4; line mean, 32–128; frame mean, 1). Single confocal planes (pinhole setting 1 or 2 AU) and a 488-nm line of an Argon laser for GFP and 543-nm laser for mRFP, were used respectively. GFP and mRFP channels were captured in the xyzt plane using sequential scan settings with an average delay time between 800-1000 ms per frame, every ~9 s. Typically 20–30 GFP/mRFP sequential scans were collected per time-lapse movie. Image sequences were processed with ImageJ and QuickTime. The time point with the highest average value of fluorescence intensity of both co-expressed proteins from the lifetime of frames recorded per movie was used to calculate co-localization using the "*Just another colocalization plugin"* JACoP plugin (NIH) which performs correlation analysis using the Pearsosn and Manders scatter plots and correlation coefficients (Bolte & Cordelieres, 2006) .

Immunofluorescence microscopy and image analysis. For immunofluorescence analysis, cells were fixed in 4% paraformaldehyde at room temperature, permeabilized and blocked with

PBS/1% BSA/0.01% Triton X-100, antibody incubations were performed in PBS/0.1% BSA. Secondary antibodies used were coupled to Alexa Fluor 488, Cy5, or TexasRed. Coverslips were mounted in DAPI-Fluoromount-G™ containing DAPI stain to highlight the cell nucleus. Images were acquired in x-y-z planes with an Axiovert 200 fluorescence microscope (Carl Zeiss Ltd) with a ×63 objective and 1.4 numerical aperture, mounted with an ApoTome.2 slider or with a Confocal microscope (TCS SP5; Leica) using an HCX Plan Apo CS 63.0× 1.40 NA oil objective. Quantification was performed on non-thresholded original orthogonal Z-projections generated in AxioVision LE software for a minimum of 25 cells per slide. Percent colocalization was determined using the JACoP plugin (NIH) and the particle size and number were quantified with the 'analyze particles' function in ImageJ (NIH) with size (pixel∧2) settings from 0.1 to 10 and circularity from 0 to 1. Representative images were processed in Adobe Photoshop CS3 software (Adobe Systems Inc.) where brightness/contrast was adjusted equally on images being compared. Organelle labeling with fluid-phase dyes was done as following: (10KDa) Dextran-Oregon Green®488 (Life technologies™) was pre-loaded into cells at a final concentration of 0.5mg/ml for 2h at 37°C prior to live cell imaging or fixation, LysoTracker -Green DND-26/-Red DND-99 (Life technologies™) was incubated at a final concentration of 100nM for 30 min at 37°C prior to live cell imaging or fixation, Pepstatin A-BODIPY® Conjugate (Life technologies™) was incubated at a final concentration of 1μM for 30 min at 37°C prior to live cell imaging or fixation, AlexaFlour® 488-Transferrin (Life technologies™) was incubated at a final concentration of 0.05mg/ml for 10 min at 37°C prior to live cell imaging or fixation. In the case of isolated lysosomes, fractions were incubated for 10 min at room temperature with primary antibodies, followed by incubation with fluorescence-conjugated secondary antibodies for an additional 10 min as previously described (Koga et al, 2010a). Labeled vesicles were recovered by centrifugation and spotted on a glass slide, fixed with 8% formaldehyde in 0.25M sucrose for

15 min, and visualized with a 100× objective and 1.4 numerical aperture in the Axiovert 2000 fluorescence microscope mounted with an ApoTome.2 slider.

Lentivirus-mediated shRNA. The following verified MISSION shRNA sequence targeting mouse PI4KB (PI4KIIIβ) gene cloned in lentiviral plasmid (pLKO.1-puro) purchased from Sigma-Aldrich were used to generate the stable PI4KIIIβ knockdown in NIH3T3 cells; (TRCN0000024763) 5'-CCGGCCTCAAAGAGAGGTTCCACATCTCGAGATGTGGAACCTCTCT TTGAGGTTTTT-3' and (TRCN0000024762) 5'-CCGGGCGAGAATTCATCAAGTCTTTCTCGA GAAAGACTTGATGAATTCTCGCTTTTT-3'. Sequences for generating PIP5K1A knockdown were; (TRCN0000024515) 5'-CCGGCCATTACAATGACTTTCGATTCTCGAGAATCGAAAGT CATTGTAATGGTTTTT-3' and (TRCN0000024517) 5'-CCGGGCCTCTGTCATGCCTGTTAAA CTCGAGTTTAACAGGCATGACAGAGGCTTTTT-3'. Sequences for generating PIP5K1B knockdown were; (TRCN0000024584) 5'-CCGGCCTCCAATCATATAGGTTAATCTCGAGAT TAACCTATATGATTGGAGGTTTTT-3' and (TRCN0000024585) 5'-CCGGCGGGCTATTACATG AATTTAACTCGAGTTAAATTCATGTAATAGCCCGTTTTT-3'. Lentiviral stocks were prepared by calcium phosphate transfection of this plasmid and the packaging vectors pMDLg/pRRE, pRSV-Rev and pMD2.VSVG into HEK-293T cells as described previously (Massey et al, 2008). Supernatants were collected over 36 to 48h, titred by plaque assay and used at a multiplicity of infection of 5 to infect cells. Except where indicated, the shRNA for PI4KIIIβ giving higher knock-down values (TRCN0000024763) is shown in the main figures, but main findings were validated at least in duplicate experiments with the other shRNA to discard outside target effects as shown in Supplementary Fig. S1E-G. Similarly the shRNA for PIP5K1A (TRCN0000024517) and PIP5K1B (TRCN0000024584) giving higher knock-down values are shown in main figures, but main findings were validated with a second shRNA to discard outside target effects (data not shown). Control cells are transduced with a lentiviral construct and subjected to the same procedures as PI4KIIIβ knock-down cells.

Secretion assay. In bulk secretion was determined by using a modification of the method described earlier (Blagoveshchenskaya et al, 2008). Cells were labeled with 200µCi/ml [^{35}S]-EXPRESS for 30 min at 37°C and then washed and chased for various times at 37°C in the corresponding unlabeled medium. To determine the kinetics of secretion, medium was collected at different times subsequent to start of the chase and proteins were precipitated with 10% TCA and the cells were lysed in RIPA buffer (50mM Tris-HCl, 150mM NaCl, 5mM ethylene glycol tetraacetic acid, containing 1% Triton X-100, 0.5% deoxycholate, and 0.1% SDS and supplemented with protease inhibitor cocktail (Roche), 2mM PMSF, and 10mM iodoacetamide, pH 7.5) at each time point. ^{35}S-labeled proteins in the media and lysates were then quantified by scintillation counting and normalized to the total amount of protein. Membrane trafficking from Golgi to the cell-surface was determined by following the transport of the green fluorescence tagged ts045-VSVG reporter. Cells growing at 37°C were transiently transfected with the ts045-VSVG-GFP plasmid and 12 h post-transfection, cells were shifted to 40°C for another 12 h to allow misfolding and retention of the fusion protein in the ER. Subsequently, cells were shifted to 20°C for 4 h to allow accumulation of the fusion protein in the TGN (PULSE). Following the pulse incubation, cells were shifted to 32°C (CHASE) to allow for trafficking of the fusion protein out of the TGN and were fixed with 4 % paraformaldehyde at 0, 15 and 45 min of the chase incubation. Golgi traffic was expressed as the percentage of decrease in fluorescence signal intensity in the Golgi region (defined by the juxtanuclear localization of the fluorescent signal normalized to area of the cell) at each chase time point. Membrane trafficking from Golgi to the lysosome was determined by following the transport of the LAMPs after a 20°C TGN block. Control and knockdown cells were plated to confluence (~200 x 10^6) in 245 mm x 245 mm tissue culture dishes (Nunc, Roskilde, Denmark) and were scraped and homogenized for isolation of lysosome-enriched fractions (*see methods described above*) after the following temperature treatments: none (cells growing in 37°C), Block (cells growing in 20°C for 4 h), Release (cells growing in Block conditions, shifted to 37°C for 2 h). Equal micrograms of the

lysosome-enriched fractions were run on an SDS-PAGE and immunoblotted for LAMPs. Delivery of LAMPs to the lysosomes upon the different temperature shifts was assessed from the densitometry of the immunoblots expressed as densitometric units for each condition.

Protein coimmunoprecipitation. Coimmunoprecipitation was done from membrane fractions solubilized in 25mM Tris (pH 7.2), 150mM NaCl, 5mM $MgCl_2$, 0.5% NP-40, 1mM DTT, 5% glycerol, and protease inhibitors (CoIP buffer) for 15 min on ice and then centrifuged for 15 min at 16,000g. Supernatant was pre-cleared with protein-A agarose and then immunoprecipitated with Protein-A agarose beads pre-coated with either PI4KIIIβ or control antibody for 2 hours at 4°C. Subsequent to three washes in CoIP buffer, the immunoprecipitates were eluted from the beads by denaturation in Laemmli buffer at 100°C for 5 min.

Measurement of PI-4-Kinase activity *in vitro.* PI-4-Kinase activity was measured as previously described (Sweeney et al, 2002). Lysosome and Golgi membranes isolated from rat liver were incubated in 20mM HEPES, pH 7.3, 125mM KCl, 2.5mM $MgCl_2$, 2mM ATP, and [γ-^{32}P] ATP at a final specific activity of 70μCi/μmol. The samples were incubated for 15 min at 37 °C, and the reactions were terminated by addition of 1N HCl followed by $CHCl_3$:MeOH (1:1). The chloroform phase was separated by centrifugation, transferred to a fresh tube, and washed with MeOH:HCl (1N) (1:1). The organic phase was vacuum-dried and resuspended in $CHCl_3$:MeOH:HCl (12 N) (200:100:1), and spotted onto TLC plates impregnated with oxalic acid. The plates were developed with $CHCl_3$:MeOH: H_2O:NH_4OH (65:47:11:1.6), and the radiolabeled phospholipids were identified by autoradiography. The different PIP species were identified using the following non-radioactive standards: PI, PI-4-P,PI-3-P,PI-5-P, PIP_2,PIP_3 and a PI-mix purchased from Avanti Polar Lipids Inc. The Rf values were calculated for each of the detected bands and matched with the corresponding standard.

Isolation of subcellular fractions. Lysosomes from rat or mouse liver and cultured cells were isolated from a light mitochondrial-lysosomal (lysosome enriched) fraction by centrifugation through a discontinuous metrizamide (Aniento et al, 1993; Bandyopadhyay et al, 2010; Cuervo et al, 1997; Koga et al, 2010b) or metrizamide/percoll discontinuous density gradient (Storrie & Madden, 1990), respectively. Purity of the lysosomal fractions was assessed by measuring total and specific enzymatic activities of mitochondrial (succinic dehydrogenase <0.01%; ornitine transcarbamilase <0.02%), peroxisomal (catalse <0.001%) and cytosolic enzymes (lactate dehydrogenase <0.01%) that constitute the only possible contaminants in these fractions. Enrichment of activity for lysosomal enzymes (β-hexosaminidase and b-n-acetyl-glycosaminidase) compared to homogenate was of 30-45%, whereas mitochondria, peroxisomal and cytosolic enzymes had enrichments <0.5-0.1 folds over the homogenate integrity of the lysosomal membrane was determine by measurement of leakage of lysosomal enzymes in the media (Storrie & Madden, 1990). Briefly, right after isolation or at the end of the incubation in the fusion buffer, lysosomes were subjected to centrifugation and the activity of the lysosomal hydrolase β-hexosaminidase was measured in both the pellet (lysosomes) and the supernatant. The enzyme present in the supernatant can only originate from lysosomal disruption, as secretion of this enzyme or permeation through the membrane is not possible. Consequently, the percentage of total β-hexosaminidase activity (pellet and supernatant) present outside lysosomes (supernatant) was used to monitor lysosomal breakage. Only preparations with more than 95% intact lysosomes, measured by β-hexosaminidase latency were used (Cuervo et al, 1997). Lysosomal matrices and membranes were separated by centrifugation after hypotonic shock (Cuervo et al, 1997; Storrie & Madden, 1990). Liver cytosol was the supernatant of three successive centrifugations (6,800g, 10 min; 17,000g, 10 min; and 100,000g, 60 min). Golgi membranes were isolated from rat liver using a modification of the procedure of Slusarewicz *et al* by centrifugation through a discontinuous sucrose gradient as

described in Sweeney *et al* (Sweeney et al, 2002). Mitochondria, microsomes and plasma membrane were isolated from rat liver using procedures specified earlier (Marzella et al, 1982a).

Isolation of cytosolic vesicles. Vesicles were isolated from 10- to 15-cm confluent plates of NIH3T3 cells and prepared using the following protocol; Cells were scraped in 1X PBS, pelleted and disrupted in homogenizing buffer (0.25M sucrose, 20mM MOPS, pH 7.3) by nitrogen cavitation (nitrogen bomb; Parr Instrument Company, Moline, IL) applying a pressure of 3500 psi for 7 min. Cell homogenate was centrifuged at 2500g for 15 min to pellet the cell debris (heavy particles, or fractions of cells) and supernatant was centrifuged at 100,000g for 60 min in a TLA 110 rotor to pellet all major organelles and was designated as 100K. The supernatant of this 100K pellet was further subjected to three successive centrifugations; 300,000g, 400,000g and 500,000g and the pellets from each of these centrifugations were collected as the 300K, 400K and 500K crude vesicular fractions, respectively. For isolation of the cytosolic vesicles from rat liver, the 100K cytosolic fraction (mentioned above) was used to further isolate the 300-500K vesicles.

Proteomic analysis. The 500K cytosolic vesicles were isolated from NIH3T3 cells using the protocol described above and were then immunoprecipitated with Dynabeads® (Life technologies™) pre-coated with PI4KIIIβ antibody. The immunoprecipitated vesicles were run on a 12% SDS-PAGE gel, which was stained with Coomassie blue, and the stained bands were excised and processed for MS/MS analysis at MS Bioworks LLC (Ann Arbor, MI) following trypsin digestion. Briefly, gel pieces were washed with 25mM NH_4HCO_3 in 50% acetonitrile, dried in a SpeedVac, reduced at 56°C for 1hr with 10mM DTT in 25mM NH_4HCO_3 and alkylated for 45 min at RT with 55mM iodoacetamide in 25mM NH_4HCO_3. Following drying in a SpeedVac, the gel pieces were digested overnight with 12.5ng/μL of trypsin at 37°C. Tryptic peptides were extracted from the gel using 60% acetonitrile and 0.2% TFA and desalted and concentrated with a C18 ZipTip (Millipore). LTQ-MS/MS sequencing was performed using a

Waters NanoAcquity HPLC system interfaced to a ThermoFisher Orbitrap Velos Pro (MS Bioworks, LLC). The sequences of each peptide were determined by database searching with MASCOT (Mowse score above the predicted identity score). The MS/MS scans were screened against NCBInr database as a first choice and then validated against SWISSPROT database. A false discovery rate (FDR) for peptide identification was assessed by decoy database searching and was adjusted to less than 1.0% for proteins and less than 1.0% for the peptides.

Electron microscopy and immunogold. Cells cultured in monolayers and isolated organelles were fixed in 2.5% glutaraldehyde in 100mM sodium cacodylate, pH 7.43, and post-fixed in 1% osmium tetroxide in sodium cacodylate followed by 1% uranyl acetate. After ethanol dehydration and embedding in LX112 resin (LADD Research Industries) BEEM capsules, ultrathin sections (0.5μm) were cut and stained with uranyl acetate followed by lead citrate and viewed with a JEOL JEM-1200EX electron microscope at 80 kV. Immunogold labeling was performed in ultrathin sections of samples fixed in 4% paraformaldehyde/0.1% glutaraldehyde in sodium cacodylate, dehydrated and embedded in Lowicryl. Grids were washed in 50mM glycine in phosphate buffered saline, blocked, either single labeled with LAMP1 or double labeled with PI4KIIIβ and LAMP1 antibody for 2 h, washed extensively and incubated with the gold-conjugated secondary antibodies (1:100) for 2 h. Control grids were incubated with the secondary antibody alone or with an irrelevant immunoglobulin G. After extensive washing, samples were fixed a second time for 5 min in 2% glutaraldehyde, washed and negatively stained with 1% uranyl acetate for 15 min. All grids were viewed on a JEOL 100CX II transmission electron microscope at 80 kV. Morphometric analysis was performed using ImageJ in 10–15 different micrographs for each condition after thresholding. Morphology of vesicular clusters was compared to lysosomes, Golgi and autophagic vacuoles using previously established criteria for these organelles (Ehrenreich et al, 1973; Marzella et al, 1982b; Wattiaux et al, 1978).

Uptake and degradation of substrate proteins by isolated lysosomes. Cytosolic proteins from mouse fibroblasts in culture were metabolically radiolabeled by incubation with [^{3}H] leucine (2□Ci/ml) at 37°C for 2 days. Radiolabeled proteins were incubated with isolated disrupted lysosomes in MOPS buffer ((10mM 3-(N-morpholino) propanesulfonic acid) (MOPS) pH 7.3, 0.3M sucrose, 1mM DTT, 4.5□M cysteine) for 30 min at 37°C, and the reactions were stopped by precipitation in acid (Kaushik & Cuervo, 2009). Proteolysis was determined as the percentage of the initial acid-insoluble radioactivity (protein) transformed into acid-soluble radioactivity (amino acids and small peptides) at the end of the incubation. Preservation of the integrity of the lysosomal membrane is essential in all these studies.

General methods. Total cellular lysates were prepared using RIPA buffer (50mM Tris-HCl, 150mM NaCl, 5mM ethylene glycol tetraacetic acid, containing 1% Triton X-100, 0.5% deoxycholate, and 0.1% SDS and supplemented with protease inhibitor cocktail (Roche), 2mM PMSF, and 10mM iodoacetamide, pH 7.5). Protein concentration was determined by the Lowry method (Lowry et al, 1951) using bovine serum albumin as a standard. Samples were run on SDS–PAGE gels, transferred to polyvinylidene fluoride or nitrocellulose membranes and after blockage with low fat-milk, incubated with primary antibodies in 3% BSA. The proteins of interest were visualized by chemiluminescence using peroxidase-conjugated secondary antibodies (KPL) in an LAS-3000 Imaging System (Fujifilm, Tokyo, Japan). Densitometric quantification of the immunoblotted membranes was performed in unsaturated blot images taken in an Image Analyzer System (FUGIFILM LAS-3000) using the Image J software (NIH). Detergent resistant regions were isolated as described before (Kaushik et al, 2006). Isoelectric focusing (IEF) was done using the Protean IEF Cell (Bio-Rad) at 20°C with rapid ramping to voltage 10000 V at a current limit of 50 μA using ReadyStrip IPG Strips with a non-linear 3–10 pH range (Bio-Rad).

Statistical analysis. All numerical results are reported as mean+S.E., and represent data from a minimum of three independent experiments unless otherwise stated. We determined the statistical significance of the difference between experimental groups in instances of single comparisons by the two-tailed unpaired Student's *t*-test of the means with Sigma Plot (Jandel Scientific) software. Differences were considered statistically significant for a value of $p < 0.05$ (denoted by an asterisk).

Supplemental references

Aniento F, Emans N, Griffiths G, Gruenberg J (1993) Cytoplasmic dynein-dependent vesicular transport from early to late endosomes. *J Cell Biol* **123:** 1373-1387

Bandyopadhyay U, Sridhar S, Kaushik S, Kiffin R, Cuervo AM (2010) Identification of regulators of chaperone-nediated autophagy. *Mol Cell* **39:** 535-547

Blagoveshchenskaya A, Cheong FY, Rohde HM, Glover G, Knodler A, Nicolson T, Boehmelt G, Mayinger P (2008) Integration of Golgi trafficking and growth factor signaling by the lipid phosphatase SAC1. *J Cell Biol* **180:** 803-812

Bolte S, Cordelieres FP (2006) A guided tour into subcellular colocalization analysis in light microscopy. *Journal of microscopy* **224:** 213-232

Cuervo AM, Dice JF (1996) A receptor for the selective uptake and degradation of proteins by lysosomes. *Science* **273:** 501-503

Cuervo AM, Dice JF, Knecht E (1997) A population of rat liver lysosomes responsible for the selective uptake and degradation of cytosolic proteins. *The Journal of biological chemistry* **272:** 5606-5615

Ehrenreich JH, Bergeron JJ, Siekevitz P, Palade GE (1973) Golgi fractions prepared from rat liver homogenates. I. Isolation procedure and morphological characterization. *J Cell Biol* **59:** 45-72

Kaushik S, Cuervo AM (2009) Methods to monitor chaperone-mediated autophagy. *Methods Enzymol* **452:** 297-324

Kaushik S, Massey AC, Cuervo AM (2006) Lysosome membrane lipid microdomains: novel regulators of chaperone-mediated autophagy. *Embo J* **25:** 3921-3933

Koga H, Kaushik S, Cuervo AM (2010a) Altered lipid content inhibits autophagic vesicular fusion. *FASEB J* **24:** 3052-3065

Koga H, Kaushik S, Cuervo AM (2010b) Inhibitory effect of intracellular lipid load on macroautophagy. *Autophagy* **6:** 825-827

Lee IH, Cao L, Mostoslavsky R, Lombard DB, Liu J, Bruns NE, Tsokos M, Alt FW, Finkel T (2008) A role for the NAD-dependent deacetylase Sirt1 in the regulation of autophagy. *Proc Natl Acad Sci U S A* **105:** 3374-3379

Lowry O, Rosebrough N, Farr A, Randall R (1951) Protein measurement with the Folin phenol reagent. *J Biol Chem* **193:** 265-275

Marzella L, Ahlberg J, Glaumann H (1982a) Isolation of autophagic vacuoles from rat liver: morphological and biochemical characterization. *J Cell Biol* **93:** 144-154

Massey AC, Follenzi A, Kiffin R, Zhang C, Cuervo AM (2008) Early cellular changes after blockage of chaperone-mediated autophagy. *Autophagy* **4:** 442-456

Puertollano R, van der Wel NN, Greene LE, Eisenberg E, Peters PJ, Bonifacino JS (2003) Morphology and dynamics of clathrin/GGA1-coated carriers budding from the trans-Golgi network. *Mol Biol Cell* **14:** 1545-1557

Sherer NM, Lehmann MJ, Jimenez-Soto LF, Ingmundson A, Horner SM, Cicchetti G, Allen PG, Pypaert M, Cunningham JM, Mothes W (2003) Visualization of retroviral replication in living cells reveals budding into multivesicular bodies. *Traffic* **4:** 785-801

Storrie B, Madden E (1990) Isolation of subcellular organelles. *Meth Enzymol* **182:** 203-225

Sweeney DA, Siddhanta A, Shields D (2002) Fragmentation and re-assembly of the Golgi apparatus in vitro. A requirement for phosphatidic acid and phosphatidylinositol 4,5-bisphosphate synthesis. *J Biol Chem* **277:** 3030-3039

Wattiaux R, Wattiaux-De Coninck S, Ronveaux-dupal MF, Dubois F (1978) Isolation of rat liver lysosomes by isopycnic centrifugation in a metrizamide gradient. *J Cell Biol* **78:** 349-368

Zhang C, Cuervo AM (2008) Restoration of chaperone-mediated autophagy in aging liver improves cellular maintenance and hepatic function. *Nat Med* **14:** 959-965